ARL 70-0126
JULY 1970

Aerospace Research Laboratories

HYPERSONIC VISCOUS INTERACTION ON CURVED SURFACES

JOHN L. STOLLERY

THE OHIO STATE UNIVERSITY RESEARCH FOUNDATION
COLUMBUS, OHIO

CONTRACT NO. F33615-67-C-1758

PROJECT NO. 7064

AIR FORCE SYSTEMS COMMAND

United States Air Force

NOTICES

When Government drawings, specifications, or other data are used for any purpose other than in connection with a definitely related Government procurement operation, the United States Government thereby incurs no responsibility nor any obligation whatsoever; and the fact that the Government may have formulated, furnished, or in any way supplied the said drawings, specifications, or other data, is not to be regarded by implication or otherwise as in any manner licensing the holder or any other person or corporation, or conveying any rights or permission to manufacture, use, or sell any patented invention that may in any way be related thereto.

Agencies of the Department of Defense, qualified contractors and other government agencies may obtain copies from the

Defense Documentation Center
Cameron Station
Alexandria, Virginia 22314

This document has been released to the

. . . . . .

CLEARINGHOUSE
U.S. Department of Commerce
Springfield, Virginia 22151

for sale to the public.

Copies of ARL Technical Documentary Reports should not be returned to Aerospace Research Laboratories unless return is required by security considerations, contractual obligations or notices on a specified document.

400-October 1970-CO405-7-71-134

ARL 70-0126

HYPERSONIC VISCOUS INTERACTION ON CURVED SURFACES

JOHN L. STOLLERY

THE OHIO STATE UNIVERSITY RESEARCH FOUNDATION
COLUMBUS, OHIO

JULY 1970

CONTRACT NO. F33615-67-C-1758
PROJECT NO. 7064

AEROSPACE RESEARCH LABORATORIES
AIR FORCE SYSTEMS COMMAND
UNITED STATES AIR FORCE
WRIGHT-PATTERSON AIR FORCE BASE, OHIO

FOREWORD

This work was undertaken during the period May - October 1969 when the author was enjoying sabbatical leave from Imperial College, London, at the Aerospace Research Laboratories, Wright-Patterson Air Force Base, Ohio.

It is a pleasure to acknowledge the enthusiastic support provided by Mr. Donald Stevens (Systems Research Laboratories, Inc.) who developed and ran the computer programs involved in this study. I am also greatly indebted to Capt James Christian who cheerfully and carefully undertook the very onerous task of converting my handwritten manuscript into an acceptable report. This report was prepared by the Hypersonic Research Laboratory of the Aerospace Research Laboratories, Air Force Systems Command, United States Air Force, under Project 7064, entitled "High Velocity Fluid Mechanics."

ABSTRACT

Cheng's analysis of strong viscous interaction between a laminar boundary layer growing over a flat plate and the external hypersonic flow field is extended to cover curved surfaces. It is demonstrated that the solutions for concave surfaces are oscillatory and physically unrealistic. The reason for this behavior is that the Busemann term in the Newton-Busemann pressure law used in Cheng's analysis over-corrects for centrifugal effects. The removal of the Busemann term or the substitution of the tangent-wedge pressure law results in a more realistic analysis which can cover both strong and weak viscous interaction over a variety of two-dimensional shapes. A number of examples are included together with comparative experimental data.

TABLE OF CONTENTS

BLANK PAGE

LIST OF FIGURES

LIST OF FIGURES (Cont'd)

NOMENCLATURE

A	$\left(\frac{\gamma-1}{2}\right) 0.664 \left(1 + 2.6 \frac{Tw}{To}\right)$
C	constant in temperature-viscosity law
Cf	skin friction coefficient
Cp	pressure coefficient
K	$M\, dy_e/dx$
k	constant
L	a characteristic length defined by equation (25)
ℓ	a characteristic length defined by equations (11) and (19)
M	Mach number
m	index of pressure variation
n	index of body shape - see e.g. equation (35)
P	p/p_∞
Pr	Prandtl number
p	static pressure
R	$\int P dx$
Re	Reynolds number
St	Stanton number
T	temperature
X	x/L
x, y	cartesian coordinates along and normal to the chord line
Y	$y/\alpha L$
z	y_e/ℓ or $y_e/\alpha\ell$
α	incidence, local surface slope or constant in description of body shape i.e. $y_w = \alpha x^n$
γ	ratio of specific heats
δ^*	boundary layer displacement thickness
ζ	x/ℓ
ξ	dummy variable, see equation (1)
$\bar{\chi}$	viscous interaction parameter $= M^3 \sqrt{C}/\sqrt{Re_x}$

Subscripts

e	edge
fp	flat plate with no viscous interaction
o	reservoir
w	wall
∞	free stream

I. INTRODUCTION

The classic paper by Cheng et al[1] laid the foundations of the problem by clearly demonstrating the mutual effects of local surface incidence and boundary layer growth. By adopting Lees' "local flat plate similarity" theory[2] for hypersonic boundary layers together with the Newton-Busemann approximation for the pressure distribution, he was able to elegantly uncover the controlling parameter for strong viscous interaction over any shape of sharp-edged surface though the only application so far has been to flat plates at incidence.

The use of the Newton-Busemann pressure law limited Cheng's analysis to strong interaction regions but any one of a number of approximate pressure relations can be used in its place. More recently, Sullivan[3] has used the tangent-wedge approximation in combination with Lees' boundary layer theory[2] to investigate the flow around a convex corner.

The aim of this paper is to apply both of the above methods to a wider variety of two-dimensional configurations, to compare and contrast the results, and to discuss them in the light of experimental data wherever possible.

II. THEORY

The local flat plate similarity solution for hypersonic boundary layers leads to the following simple results (Pr = 1):

$$\frac{M\delta^*}{x} = \frac{\gamma-1}{2} \cdot 0.664 \left(1 + 2.6\frac{Tw}{To}\right) \bar{\chi}\left[\int_0^x \frac{p}{p_\infty} \cdot \frac{d\xi}{x}\right]^{1/2}\left(\frac{p}{p_\infty}\right)^{-1} \tag{1}$$

$$\equiv A\bar{\chi}\left[\int_0^x P\frac{d\xi}{x}\right]^{1/2} P^{-1} \tag{1a}$$

$$M^3\,St = 0.332\,\bar{\chi}\,P\left[\int_0^x P\frac{d\xi}{x}\right]^{-1/2} \tag{2}$$

$$C_f \simeq 2\,St \tag{3}$$

where

$$\bar{\chi} = M^3\sqrt{\frac{C}{Re_x}} \quad . \tag{4}$$

Values of the constants for other Prandtl numbers have been quoted by Dewey[4] and Sullivan[5].

If the pressure distribution can be expressed in terms of the effective body shape, $y_e(x)$,

as

$$P = P(y_e) \tag{5}$$

where

$$y_e = y_w + \delta^* \tag{6}$$

then Eqs. (1), (5), and (6) can be solved for P, y_e, and δ^* once the surface shape $y_w(x)$ is specified.

A. THE NEWTON-BUSEMANN LAW

Cheng used the Newton-Busemann relation for the pressure distribution i. e.

$$p = \gamma\, p_\infty M^2 (y_e'^2 + y_e\, y_e'') = \gamma\, p_\infty M^2 (y_e\, y_e')' \tag{7}$$

which when substituted in (1) gives

$$(y_e - y_w)\left\{\sqrt{y_e y_e'}\right\}' = \sqrt{\frac{A^2\bar{\chi}^2 x}{4\gamma M^4}} \equiv B \text{ say.} \tag{8}$$

This is identical to Cheng's result with the minor error of omission of γ from the denominator repaired. Equation (8) is the fundamental equation for y_e given any shape of wall: a number of examples will be considered. Since B is a constant, the equation may be scaled to make $B = 1$.

1. Flat Plate (Strong Interaction)

If $y_w = 0$ then writing

$$z = y_e/\ell \quad \text{and} \quad \zeta = x/\ell \tag{9}$$

converts (8) to

$$z\left(\sqrt{zz'}\right)' = 1 \tag{10}$$

provided

$$\ell = \frac{A^2\bar{\chi}^2 x}{4\gamma M^4} \tag{11}$$

Substitution of $z = k\zeta^m$ in (10) shows that the equation is satisfied for $m = 3/4$ and $k = 2\sqrt{2}/3^{1/4}$ yielding the familiar strong interaction results:

$$\frac{M\delta^*}{x} = \frac{2}{(3\gamma)^{1/4}}(A\bar{\chi})^{1/2}, \tag{12}$$

$$\frac{p}{p_\infty} = \sqrt{\frac{3\gamma}{4}} \cdot A\bar{\chi}, \tag{13}$$

and

$$\frac{St}{St_{fp}} = \frac{(3\gamma)^{1/4}}{2}(A\bar{\chi})^{1/2}, \tag{14}$$

where $$A = \left(\frac{\gamma-1}{2}\right) 0.664 \left(1 + 2.6 \frac{T_w}{T_o}\right) \tag{15}$$

and

$$St_{fp} = 0.332 \sqrt{C/Re_x} \quad . \tag{16}$$

The weak interaction result does not satisfy the Newton-Busemann relation and hence is not a solution of (10).

2. Surfaces Described by $y_w = kx^n$

The family of shapes

$$\frac{y_w}{a\ell} = \left(\frac{x}{\ell}\right)^n \quad \text{or} \quad z = \zeta^n \tag{17}$$

is of some interest and includes the flat plate at incidence ($n = 1$). Equation (8) may be written as

$$(z - \zeta^n) \left(\sqrt{zz'}\right)' = 1 \tag{18}$$

provided that

$$\ell = \frac{A^2 \bar{\chi}^2 x}{4\gamma M^4 a^4} \tag{19}$$

In terms of the new variables the required physical quantities are

$$\frac{\delta^*}{a\ell} = (z - \zeta^n) \tag{20}$$

$$\frac{p}{\gamma p_\infty M_\infty{}^2 a^2} = (zz')' \tag{21}$$

and

$$\frac{ASt}{0.332\, a^3 4\gamma} = \left(\frac{1}{z - \zeta^n}\right) \tag{22}$$

Thus from the scaling (Eq. 19) Cheng's analysis highlights the parameter $(M^2 a^2 / A \bar{\chi})$ which controls the relative importance of the effects of

incidence and strong interaction (displacement).

B. THE TANGENT-WEDGE APPROXIMATION

The scope of the theoretical analysis can be extended by using an alternative pressure law which is capable of embracing both the strong and weak interaction regions. For example, a modified Newtonian law could be used of the form

$$P = \frac{p}{p_\infty} = 1 + \gamma M^2 y_e'^2 = 1 + \gamma K^2 \tag{23}$$

One of the more successful approximations at hypersonic speeds is the tangent-wedge rule and Sullivan has used this in place of the Newton-Busemann law employed by Cheng.

The boundary layer equation (see (1)) may be written as

$$\frac{M\delta^*}{L} = A\bar{\chi}\sqrt{\frac{x}{L}}\sqrt{\frac{R}{P}} \tag{24}$$

and if L is chosen such that

$$L = A^2\bar{\chi}^2 x \tag{25}$$

then

$$X = x/L = (A\bar{\chi})^{-2} \tag{26}$$

and

$$\frac{M\delta^*}{L} = \sqrt{\frac{R}{P}} \tag{27}$$

where

$$\frac{dR}{dX} = P \tag{28}$$

The tangent wedge rule is

$$P = 1 + \gamma K^2\left[\frac{\gamma+1}{4} + \left\{\left(\frac{\gamma+1}{4}\right)^2 + \frac{1}{K^2}\right\}^{1/2}\right] \tag{29}$$

or

$$K = \frac{P-1}{\gamma\left\{1 + \left(\frac{\gamma+1}{2\gamma}\right)(P-1)\right\}^{1/2}} \tag{30}$$

where $$K = M\frac{dy_e}{dx} = M\left(\frac{d\delta^*}{dx} + \frac{dy_w}{dx}\right) \tag{31}$$

From (27)

$$M\frac{d\delta^*}{dx} = \frac{1}{2R^{1/2}} - \frac{R^{1/2}}{P^2}\cdot\frac{dP}{dX} \tag{32}$$

Eliminating $d\delta^*/dx$ from the last pair of equations and substituting for K leads to the final result.

$$\frac{dP}{dX} = \frac{P^2}{2R}\left\{1 + 2R^{1/2}\left[M_\infty\frac{dy_w}{dx} - \frac{(P-1)}{\gamma\left\{1+\frac{\gamma+1}{2\gamma}(P-1)\right\}^{1/2}}\right]\right\} \tag{33}$$

$$\frac{dR}{dX} = P \tag{34}$$

Equations (33) and (34) can be solved for P(x), R(x), and then $\delta^*(x)$ from (24) once y_w is specified.

C. TANGENT-WEDGE APPROXIMATION APPLIED TO SURFACES DESCRIBED BY $y_w = kx^n$

For a family of shapes

$$\frac{y_w}{L} = a\left(\frac{x}{L}\right)^n \tag{35}$$

or

$$Y_w = X^n \quad \text{where} \quad Y_w = y_w/aL \quad \text{and} \quad X = x/L \tag{36}$$

the equations to solve become

$$\frac{dP}{dX} = \frac{P^2}{2R}\left\{1 + 2R^{1/2}\left[M_\infty a\frac{dY_w}{dX} - \frac{(P-1)}{\gamma\sqrt{1+\frac{\gamma+1}{2\gamma}(P-1)}}\right]\right\} \tag{37}$$

and $$\frac{dR}{dX} = P \tag{34}$$

For the particular case of a flat plate at zero incidence $dY_w/dX = 0$. Substitution of $P = kX^m$ with $P >> 1$ in (34) and (37) enables k and m to be evaluated as

$$P = \frac{3\sqrt{\gamma(\gamma+1)}}{4} \cdot A\bar{\chi} \tag{38}$$

which is identical to the result given by Cox and Crabtree[6]. The use of the modified Newtonian rule (see (23)) would have given

$$P = \frac{3\sqrt{\gamma}}{2\sqrt{2}} \cdot A\bar{\chi} \tag{39}$$

The weak interaction condition is also satisfied since from (37)

$$\frac{dP}{dX} \to \frac{1}{2X} \quad \text{as} \quad P \to 1, \quad \text{i.e.} \quad \frac{dP}{dX} \to 0 \quad \text{as} \quad X \to \infty .$$

III. RESULTS

The governing equations for both theories have been solved for a variety of surfaces including the flat plate at both positive and negative incidence (n = 1), concave and convex plates (n = 2, 3), and compression and expansion corners. The numerical results were obtained by digital machine computation using an IBM 7094 and FORTRAN IV language. A standard 3rd order Runge-Kutta technique was adopted with double precision arithmetic and a fixed step size of 10^{-4}.

A. FLAT PLATE AT ZERO INCIDENCE

Comparisons between the various theories and some experimental data are shown in Figs. 1 and 2. As mentioned earlier, Cheng's theory is for strong interaction only, but it immediately indicates the importance of the parameter $A\overline{\chi}$ provided the leading edge is sharp. First order strong and weak viscous interaction theories give a reasonable indication of the flow development with the changeover from strong to weak interaction occurring near $A\overline{\chi} = 1.5$. The use of the tangent wedge rule for pressure gives a smooth transition from strong to weak interaction and the agreement with some experimental data taken from Ref. 7 is reasonably good.

B. FLAT PLATE AT INCIDENCE

The pressure distribution over a wedge (α positive) as calculated using the method of Cheng and Sullivan is shown in Fig. 3. Cheng's result shows that near the leading edge the displacement effect is dominant and the pressure distribution is identical to that on a flat plate at zero incidence. Further downstream the incidence effects increase in importance and eventually the curve "peels off" towards the inviscid limit

$$\frac{P}{\gamma M^2 \alpha^2} = 1 \tag{40}$$

Cheng's result holds for all $M\alpha$ provided that the shock is strong. Recently Kemp[8] has reported some tests in helium at $M = 42$ which show that Cheng's theory predicts the trends quite well under these conditions.

If the tangent wedge approximation is used, then there is a different solution for every $M\alpha$ and the asymptotic pressure level is

$$\frac{P}{\gamma M^2 \alpha^2} = \left\{ \frac{\gamma+1}{4} + \left[\left(\frac{\gamma+1}{4} \right)^2 + \frac{1}{M^2 \alpha^2} \right]^{1/2} \right\} + \frac{1}{\gamma M^2 \alpha^2} \qquad (40a)$$

This will only tend to Cheng's value for $M_\infty \alpha >> 1$. Because of these differing asymptotes, the curves look dissimilar. A more realistic comparison can be achieved either by interpreting Cheng's result as $P - P_{wedge}$ so that his asymptotic value becomes

$$P_{wedge} = 1 + \gamma M^2 \alpha^2 \qquad (41)$$

or by plotting all the results as

$$\frac{P - P_{wedge}}{\gamma M^2 \alpha^2} + 1$$

Presented in this way, the curves compare well (Fig 4).

The heat transfer rates calculated by the two methods are similar, the agreement improving as $M\alpha$ is increased (Fig 5). Cheng's results show that it isn't until $M^2 \alpha^2 / A\bar{\chi}$ is of order unity that large deviations from the zero incidence condition occur. The flat plate value can be expressed as

$$\frac{A\,St}{0.332 \cdot 4\gamma\, \alpha^3} = \frac{(3\gamma)^{1/4}}{8\gamma} \cdot \left\{ \frac{M^2 \alpha^2}{A\bar{\chi}} \right\}^{-3/2} \qquad (42)$$

Similar remarks apply to the negative incidence results. Any calculations made using Cheng's method must show the pressure distribution tending asymptotically to zero, whereas the tangent wedge limit is given by

$$P = 1 + \gamma M^2 a^2 \left\{ \frac{\gamma+1}{4} - \left[\left(\frac{\gamma+1}{4} \right)^2 + \frac{1}{M^2 a^2} \right]^{1/2} \right\} \tag{43}$$

Since P cannot be negative, the lowest permissible value of Ma is $-\sqrt{2/\gamma(\gamma-1)}$. Of course, the range of the calculations could be extended by using a more suitable pressure law for expansive flows.

C. CONCAVE SURFACES ($y_w = kx^n$; n = 2, 3)

The most striking feature of Cheng's results for these bodies is the oscillatory behavior of the boundary layer. The boundary layer, dominated near the leading edge by displacement effects, grows initially as though supported by a flat plate. Faced with the adverse pressure gradient downstream the boundary layer thins dramatically to a "neck," then widens again and the cycle of events is repeated. Beneath each "neck" the pressure and heat transfer rate reach local peaks. This pattern of behavior is similar in character to, but much more severe in magnitude than that found experimentally; it appears that the Busemann centrifugal correction is far too powerful in the assumed pressure law. As the flow moves around the surface, the dominant influence changes from displacement to incidence and the pressure should approach the inviscid value

$$P = \gamma M^2 a^2 (zz')' \tag{44}$$

For n = 2 ($z = \zeta^2$) this relationship implies that

$$\frac{P}{\gamma M^2 a^2} = 6\zeta^2 = 96\gamma^2 \left\{ \frac{M^2 a^2}{A\bar{X}} \right\}^4 \tag{45}$$

and as Fig. 6 shows, the pressure distribution does, in fact, oscillate about this line for large x. Similar remarks apply to the cubic surface, the "final pressure" oscillating around

$$\frac{P}{\gamma M^2 a^2} = 3840\ \gamma^4 \left\{ \frac{M^2 a^2}{A\bar{X}} \right\}^8 \tag{46}$$

When the more realistic tangent-wedge approximation is used then there is no oscillation, the boundary layer thickness decreasing steadily as the pressure rises. As a further check, the modified Newtonian pressure distribution

$$P = 1 + \gamma K^2 \tag{47}$$

was used to calculate the flow around the quadratic surface and the result is also plotted on Fig 6. There is no oscillatory behavior and the numerical values are close to those calculated using the tangent wedge law.

Figure 7 shows the corresponding heat transfer rate distributions for the body $y_w = ax^2$. Values calculated using Cheng's method oscillate about the limiting value ($y_e \rightarrow y_w$) which for this shape of body is

$$\frac{A\,St}{0.332 \cdot 4\gamma \cdot a^3} = \left(6\sqrt{\gamma/2}\right)\left(\frac{M^2\,a^2}{A\bar{X}}\right) \tag{48}$$

In contrast the values calculated using either the tangent-wedge or modified Newtonian pressure laws are well behaved, approach the asymptotic value smoothly, and are physically more realistic.

Two theoretical predictions of boundary layer growth over a cubic surface ($y_w = x^3/150$) are compared with an estimate made from a schlieren picture of the flow in Fig 8. The "pulsating" thickness predicted by Cheng's method is clearly shown with the outer edge coming very close to the wall at the first "neck." The estimate using the tangent-wedge law is more realistic with the layer thinning slowly but continuously in the downstream region. Both estimates describe broadly the main features of the flow. Near the leading edge the displacement effect is dominant and the layer grows much as it would over a flat plate. Then, as the surface slope increases, so the incidence effect grows in importance and the shape of the outer edge of the layer approaches

that of the wall. The approximate estimate of boundary layer thickness taken from a schlieren picture confirms these trends. The favorable comparison between measured and estimated pressure distributions is shown in Fig 9.

D. CONVEX SURFACES

For convex surfaces Cheng's method is not oscillatory, the boundary layer growing rapidly but smoothly in the helpful pressure gradient. Since the Newton-Busemann law is used, the theory can only apply if y_e' is positive, i.e., in regions close to the leading edge or where the negative body slope is small.

Figure 10 compares the pressure distribution over three surfaces of the family $z = -\zeta^n$ where $n = 1$, 2 and 3.

E. FLOW PAST COMPRESSION CORNERS

As now expected, Cheng's method predicts an oscillatory behavior more violent than that found experimentally. Therefore, only the method suggested by Sullivan has been used to compare some theoretical predictions with experimental data. Comparisons have been made with three sets of pressure and heat transfer rate data at $M = 9.7$, and 20, (Figs 11(a)-(c)). Considering the simplicity of the mathematical model and the closeness of the experimental flows to incipient separation, the agreement between prediction and measurement is encouraging. It is noticeable in many of the comparisons that the predictions "lag" on the measurements in regions of strong pressure gradient. This may be due in part to the inability of the mathematical model to recognize either upstream influence or the presence of normal pressure gradients.

F. FLOW PAST EXPANSION CORNERS

Both methods are applied to an expansion corner in Fig 12 and both give predictions which are in reasonable agreement with the experimental data. The calculation using Sullivan's method is particularly good over the wedge-surface ahead of the corner. Both methods predict the rapid drop in pressure just downstream of the corner and the subsequent very slow decline towards the final level. The comparison further shows how in practice the influence of the corner feeds upstream, an effect which neither theory can predict, and how erroneous the inviscid pressure distribution is under these test conditions. Considering how nonsimilar the experimental profiles were downstream of the corner the predictions are surprisingly good.

IV. CONCLUSIONS

Lees "local flat plate similarity" method for calculating boundary layer growth can be combined with any one of a number of approximate pressure laws linking pressure to the slope of the effective body (body plus displacement thickness) to estimate the effect of viscous interaction on any two-dimensional surface. If the Newton-Busemann law is used as Cheng did, then the results are often oscillatory and physically unrealistic, though the importance of the parameter $(M^2\alpha^2 / A\overline{\chi})$ is immediately highlighted. If the tangent wedge rule is employed (as Sullivan did to examine the flow downstream of an expansion) or even the modified Newtonian rule, then the results are sensible and predict the main features of the flow very well.

This method should work well when the boundary layer profiles are reasonably similar. Its accuracy must decrease as separation conditions are approached and of course this technique can give no indication of either separation or upstream influence.

Comparisons between predictions and experimental data over a wide variety of conditions give confidence in the use of the mathematical model for initial design purposes.

REFERENCES

1. Cheng, H. K.; Hall, J. G.; Golian, T. C., and Hetzberg, A., "Boundary-Layer Displacement and Leading-Edge Bluntness Effects in High-Temperature Hypersonic Flow," J. Aero. Sci., Vol. 28, No. 5, p. 353, (May 1961).
2. Lees, L., "Laminar Heat Transfer Over Blunt Nosed Bodies at Hypersonic Flight Speeds," Jet Propulsion, Vol 26, No. 4, p. 259, (April 1956).
3. Sullivan, P. A., "On the Interaction of a Laminar Hypersonic Boundary Layer and a Corner Expansion Wave," AIAA Paper No 69-137, (January 1969).
4. Dewey, C. F., Jr., "The Use of Local Similarity Concepts in Hypersonic Viscous Interaction Problems," AIAA. J. Vol 1, No 1, p. 20, (January 1963).
5. Sullivan, P. A., "On the Interaction of a Laminar Hypersonic Boundary Layer and a Corner Expansion Wave," Univ. of Toronto, UTIAS Tech. Note 129, (August 1968).
6. Cox, R. N. and Crabtree, L. F., Elements of Hypersonic Aerodynamics, English Universities Press, London, (1965).
7. Hayes, W. D. and Probstein, R. F., Hypersonic Flow Theory, Academic Press, New York, (1959).
8. Kemp, J. H., Jr., "Hypersonic Viscous Interaction on Sharp and Blunt Enclosed Plates," AIAA. J. Vol 7, No 7, p. 1280, (July 1969).
9. Needham, D. A., "Laminar Separation in Hypersonic Flow" London University Ph. D. Thesis, (August 1965).
10. Holden, M. S., "Theoretical and Experimental Studies of Laminar Flow Separation on Flat Plate-Wedge Compression Surfaces in the Hypersonic Strong Interaction Regime," ARL 67-0112, (May 1967).
11. Stollery, J. L., "Hypersonic Viscous Interaction - An Experimental Investigation of the Flow over Flat Plates at Incidence and Around an Expansion Corner," ARL 70-0125, July 1970.

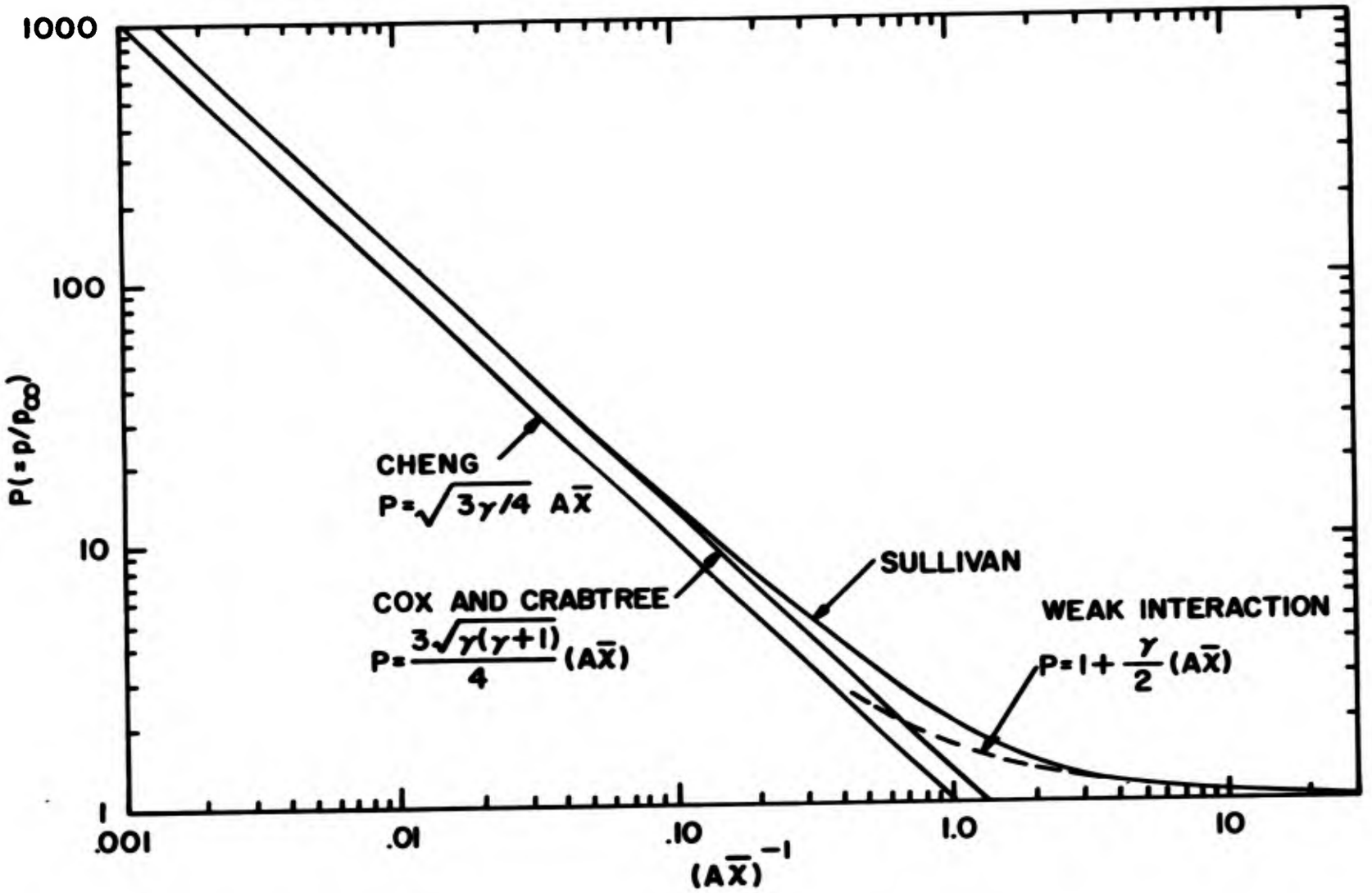

Figure 1 A comparison between theoretical estimates of the pressure distribution induced on a sharp flat plate at zero incidence.

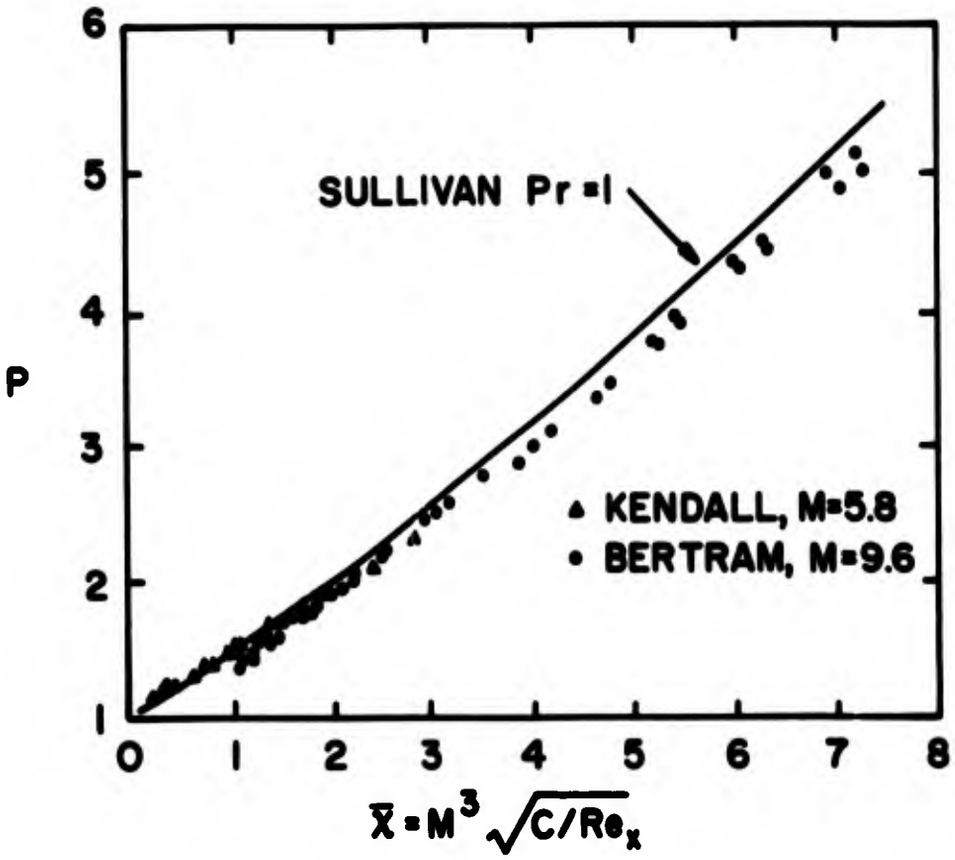

Figure 2 Weak and strong interaction on an insulated flat plate in air.

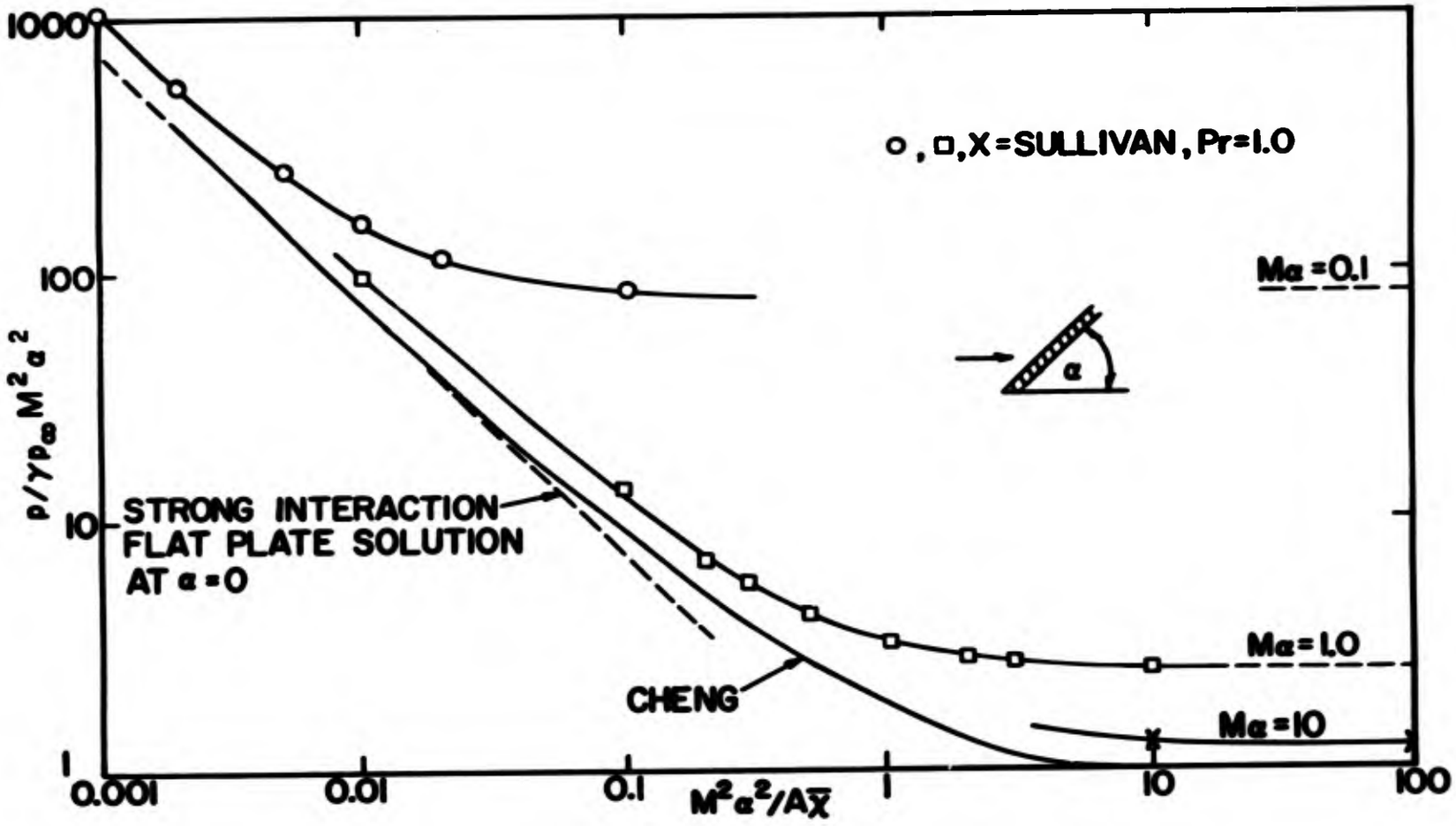

Figure 3 Predictions of the pressure distribution on a flat plate at positive incidence.

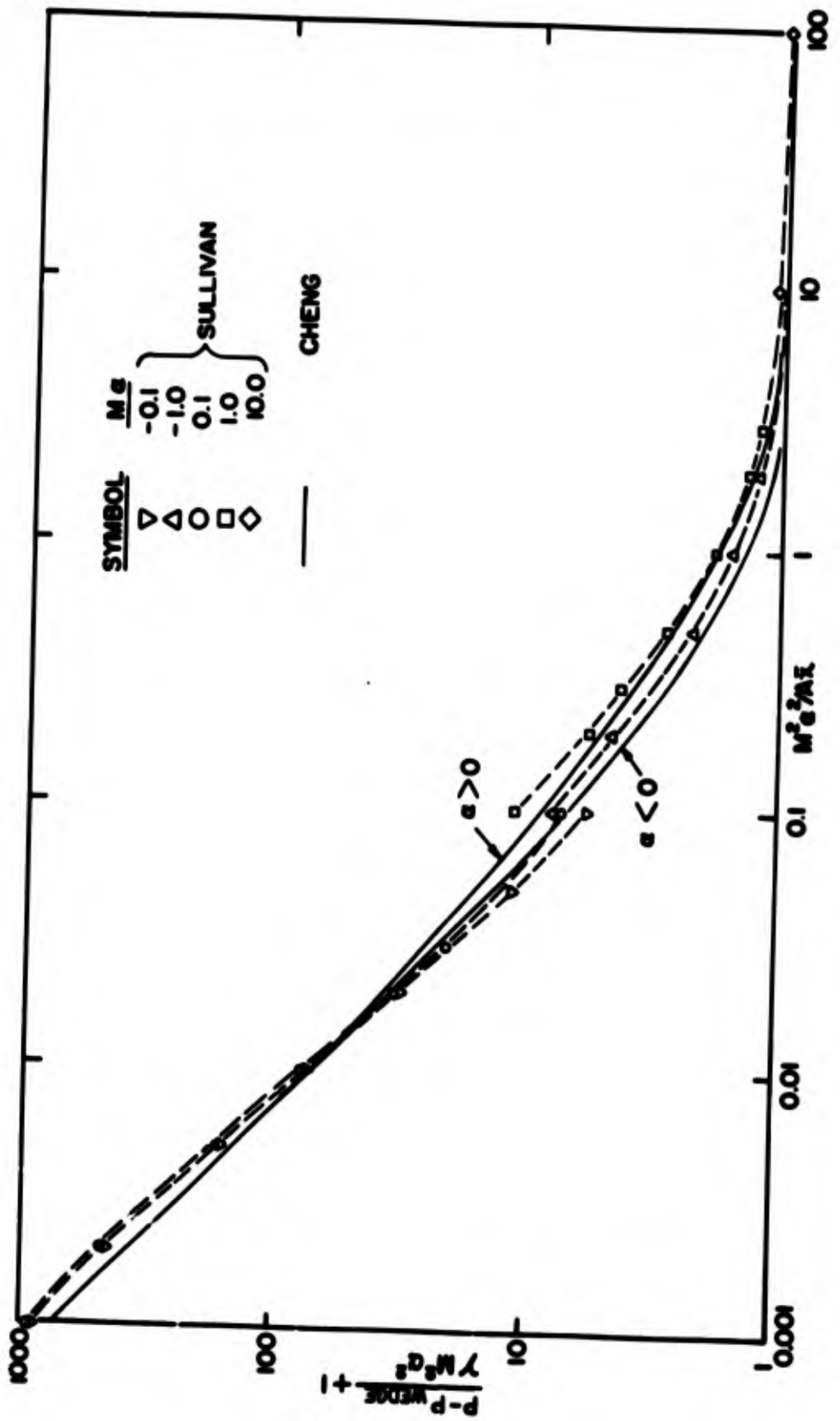

Figure 4 Pressure distribution on flat plates at positive and negative incidence.

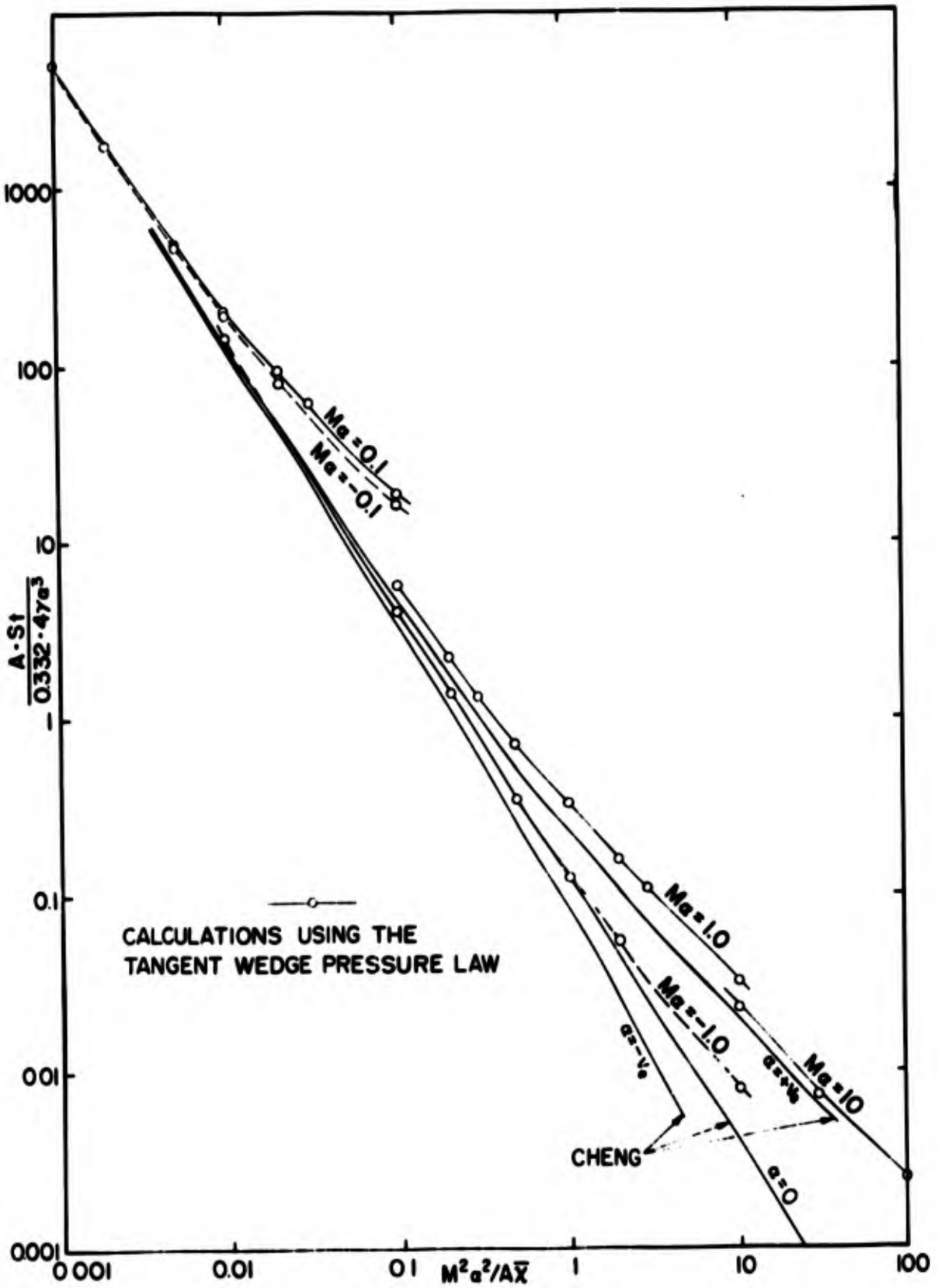

Figure 5 **Heat transfer on a flat plate at positive and negative incidence.**

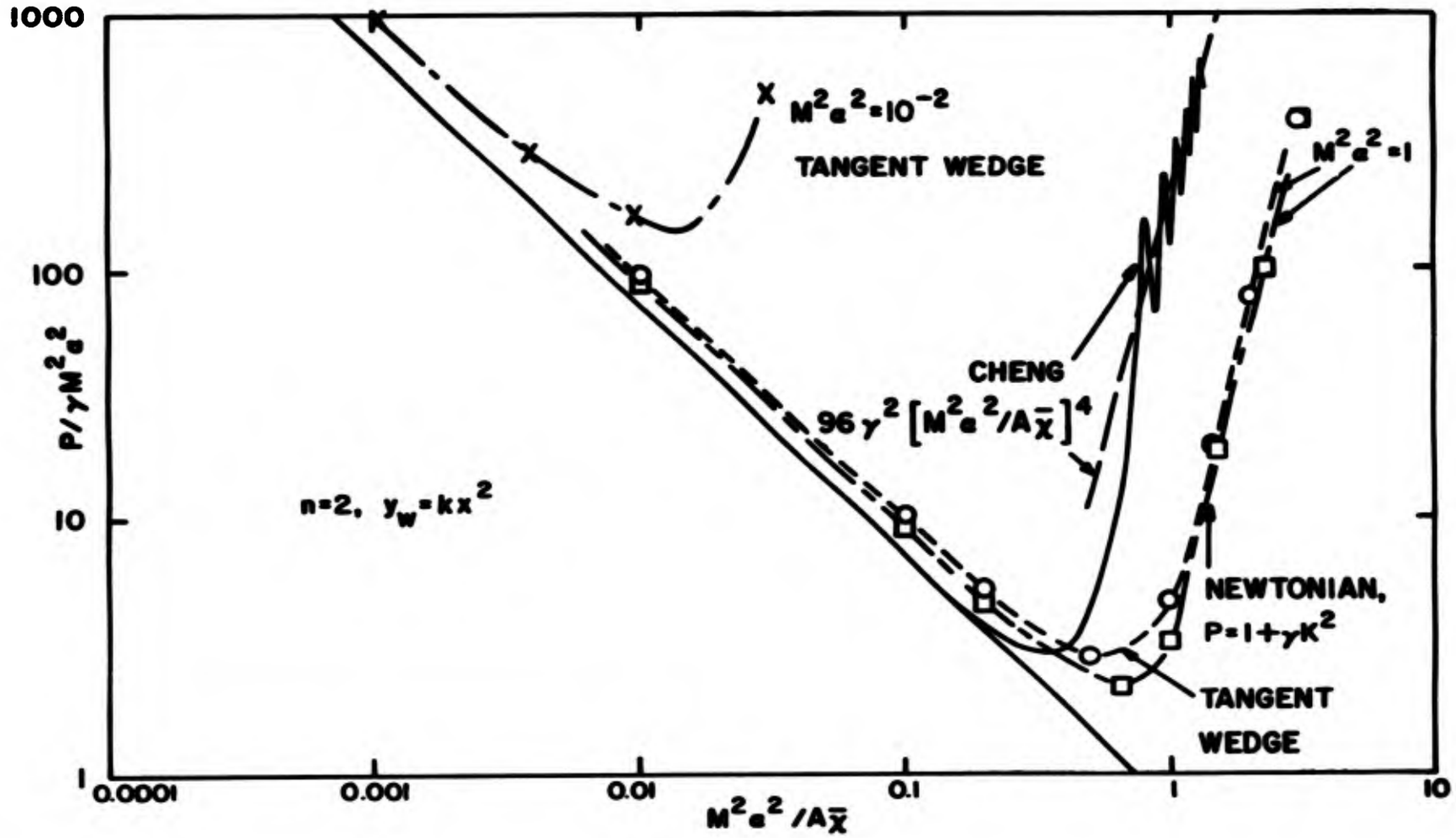

Figure 6 Pressure distribution on a concave surface of the form $y_w = kx^2$.

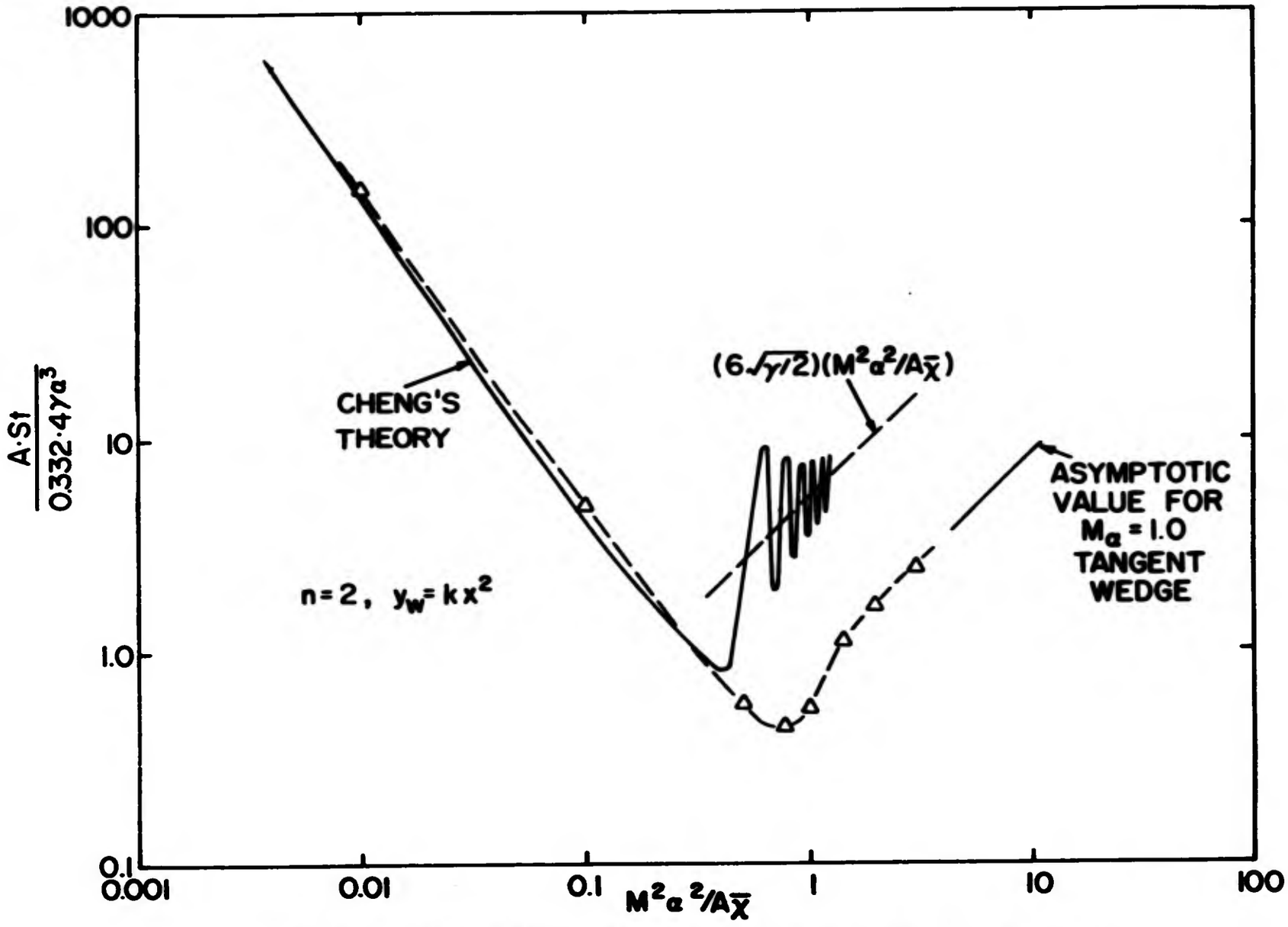

Figure 7 Heat transfer to a concave surface of the form $y_w = kx^2$.

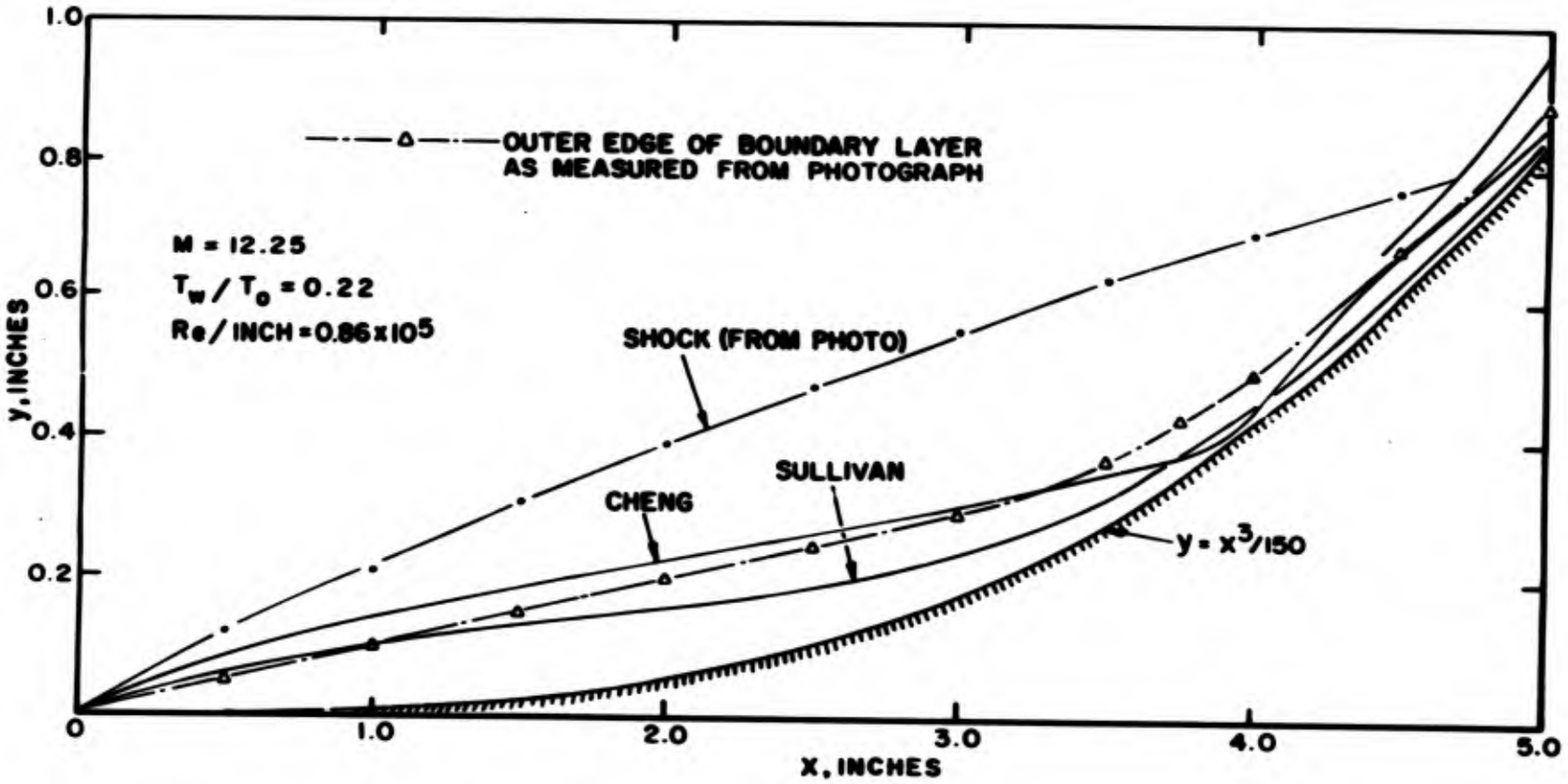

Figure 8 Boundary layer growth over a cubic body; $y = x^3 / 150$.

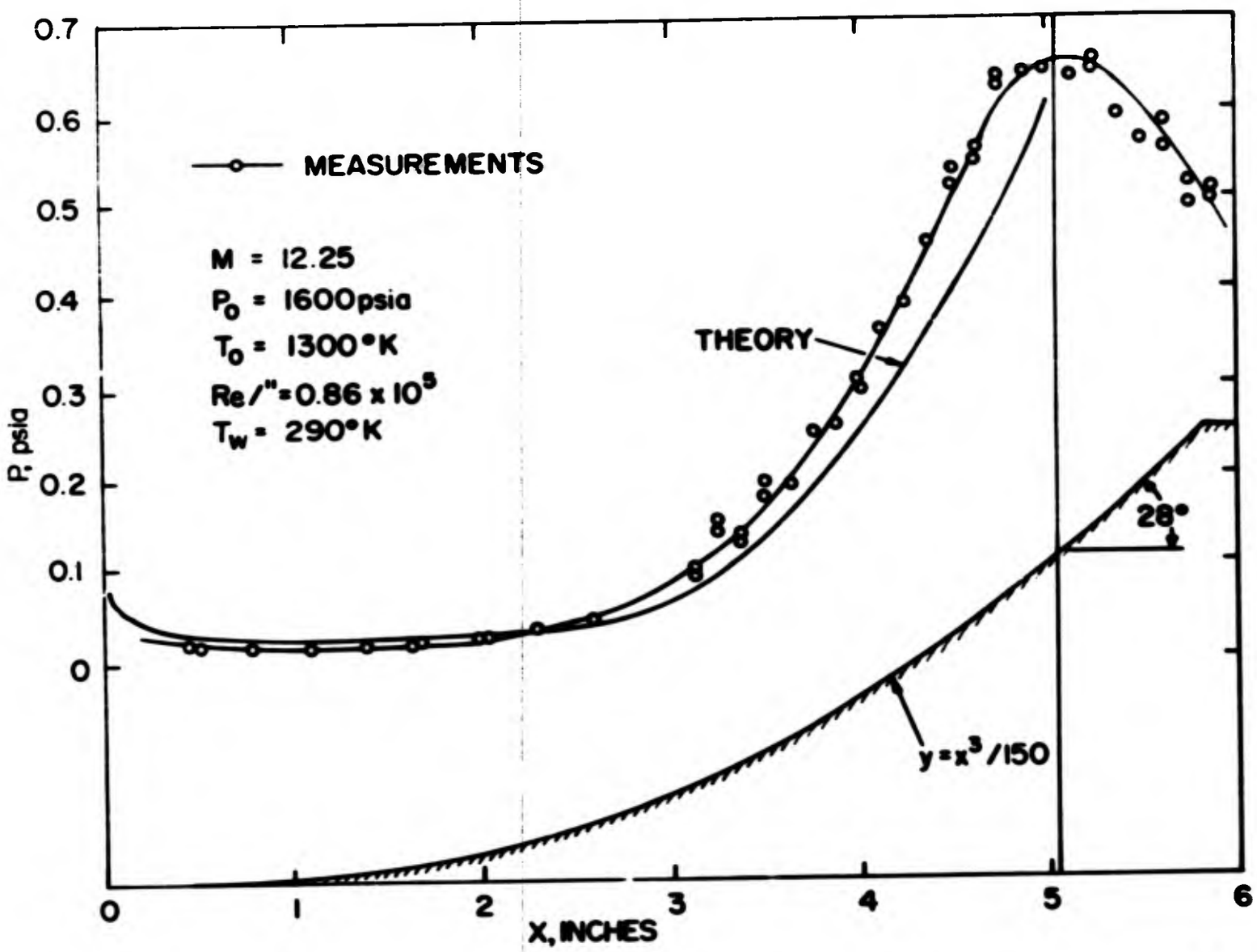

Figure 9 Pressure distribution on the cubic surface, $y = x^3/150$, $0 \leq x \leq 5.1"$.

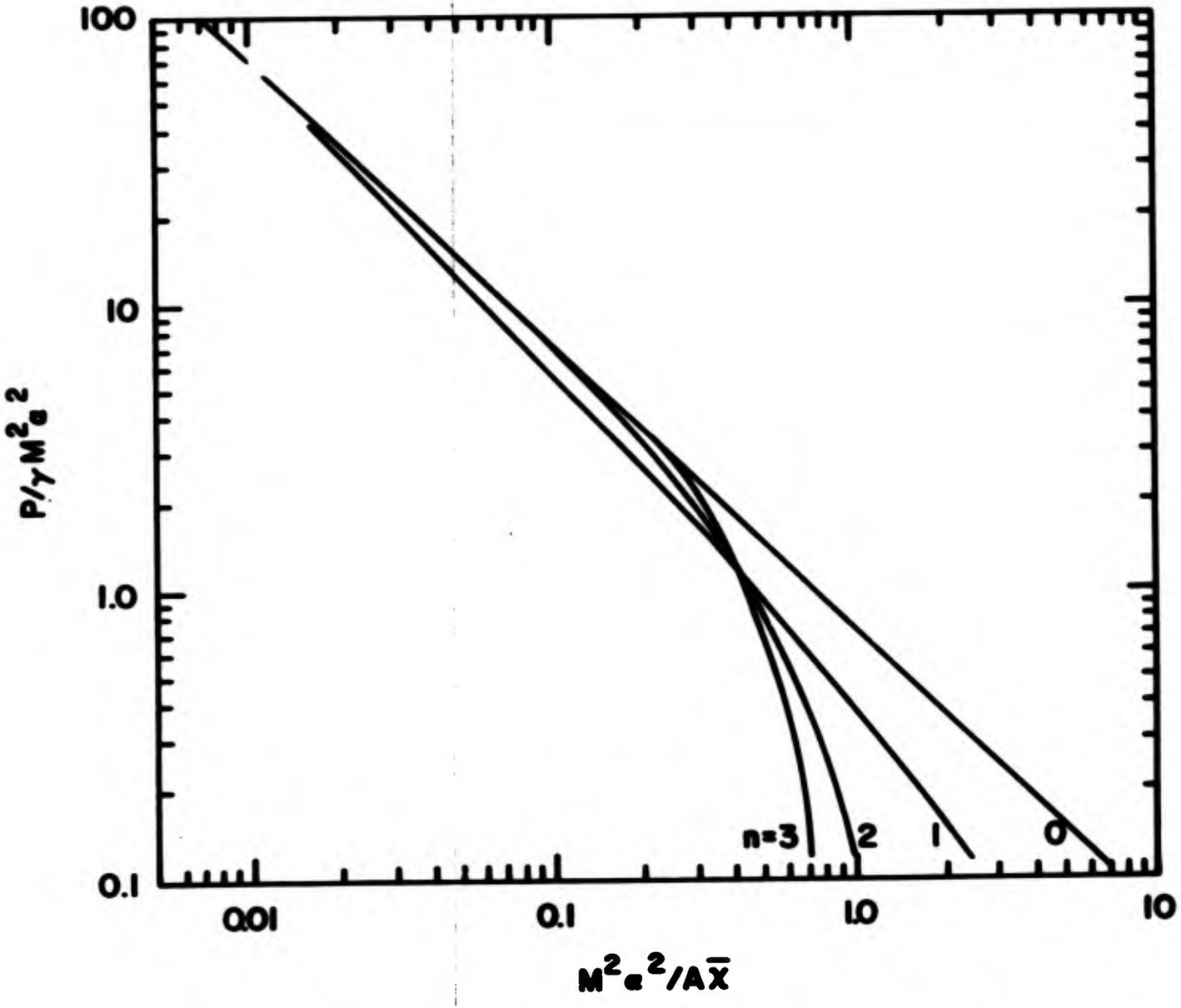

Figure 10 Theoretical pressure distribution on concave surfaces of the form $y_w = -kx^n$; n = 0, 1, 2, and 3.

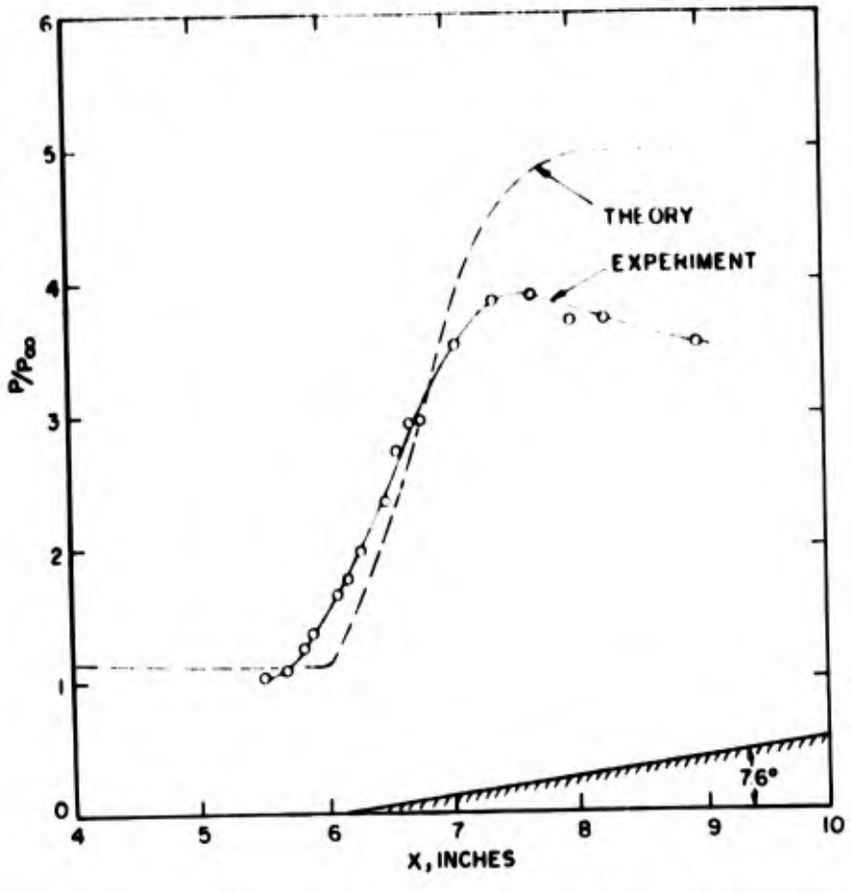

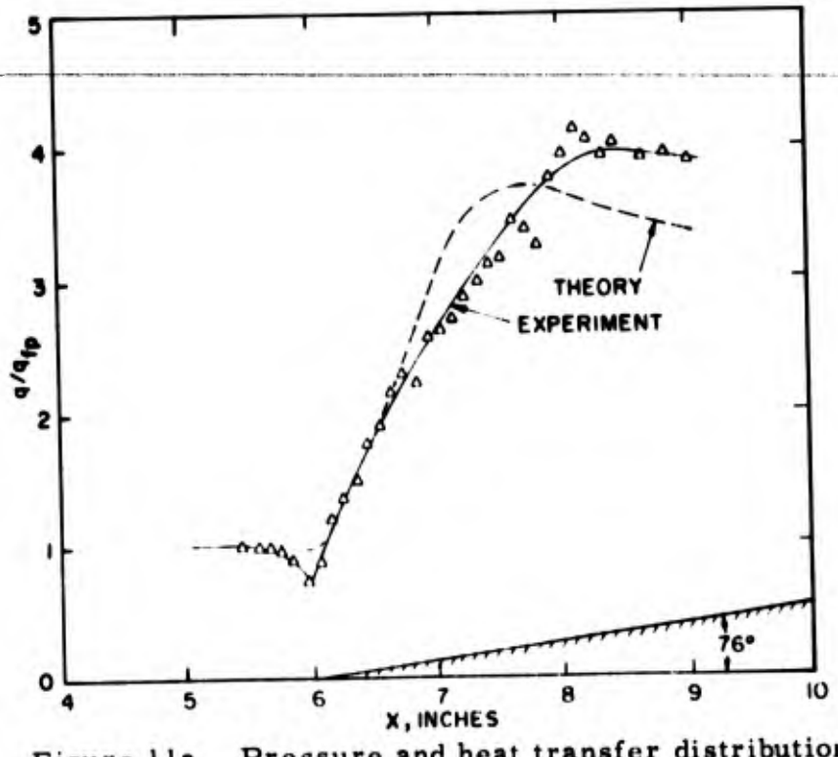

Figure 11a Pressure and heat transfer distribution on a wedge compression corner at a $M = 9.7$, $Re/" = 1.59 \times 10^5$, $\bar{X}_{HL} = 0.87$, $Tw/To = 0.22$ (Experimental data from Ref 9).

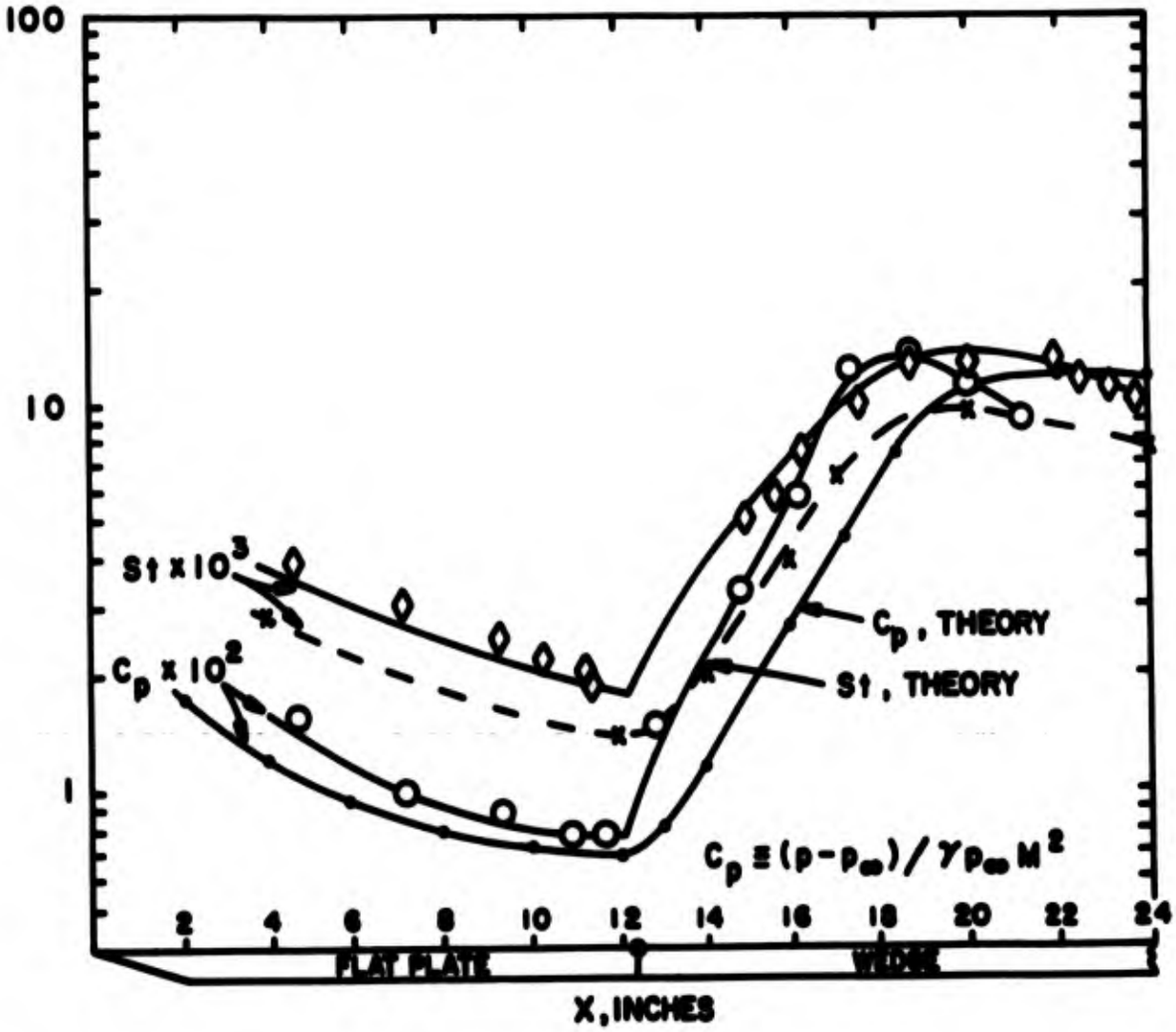

Figure 11b Pressure and heat transfer distribution on a wedge compression corner at M = 20, $\alpha_{wedge} = 16^{\circ}$, Tw/ To = 0.06, $\bar{X}_{HL} = 19.8$ (Experimental data from Ref 10).

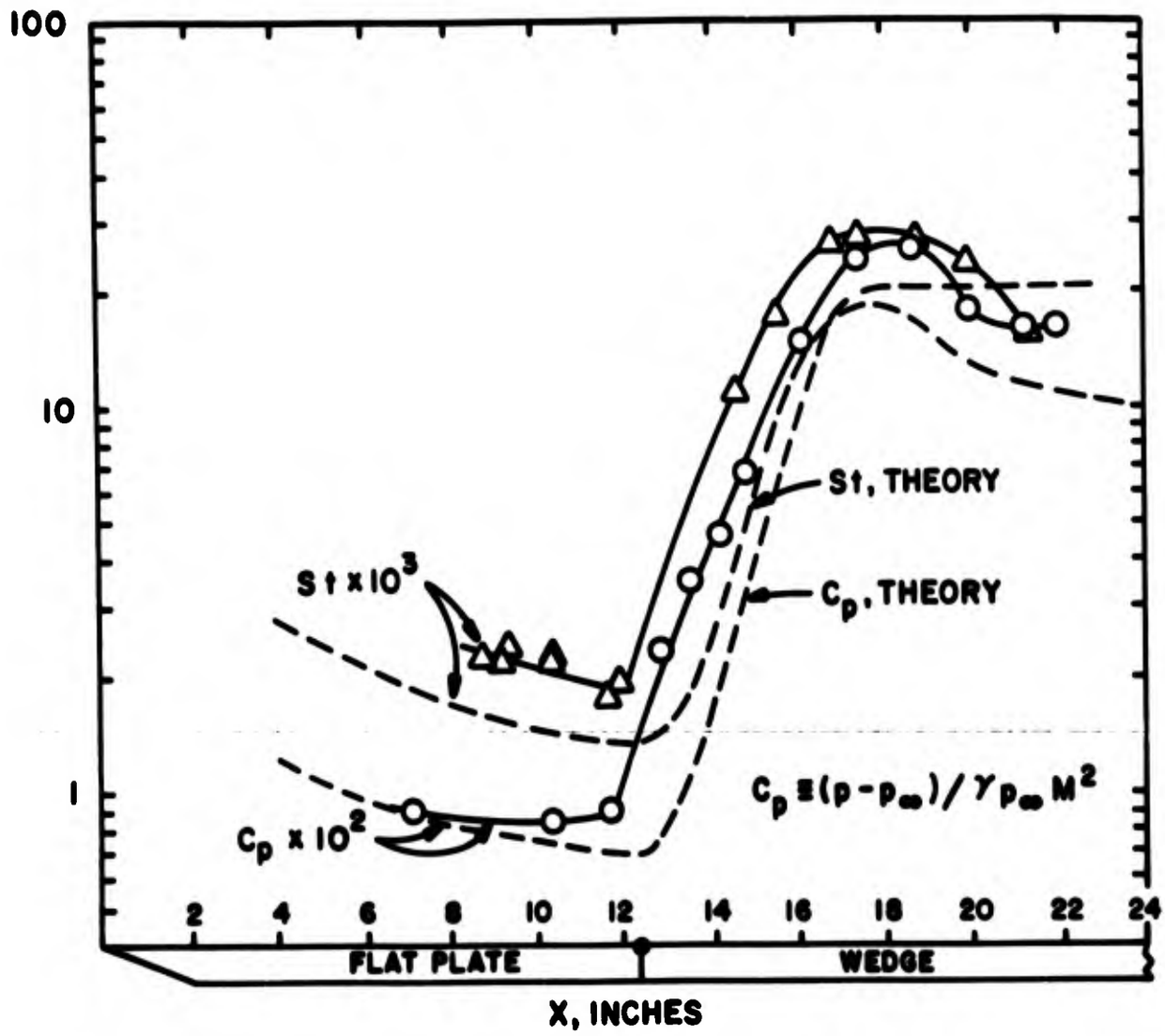

Figure 11c Pressure and heat transfer distribution on a wedge compression corner at M = 20, $\alpha_{wedge} = 21^o$, Tw/ To = 0.06, $\bar{\chi}_{HL} = 19.8$ (Experimental data from Ref 10).

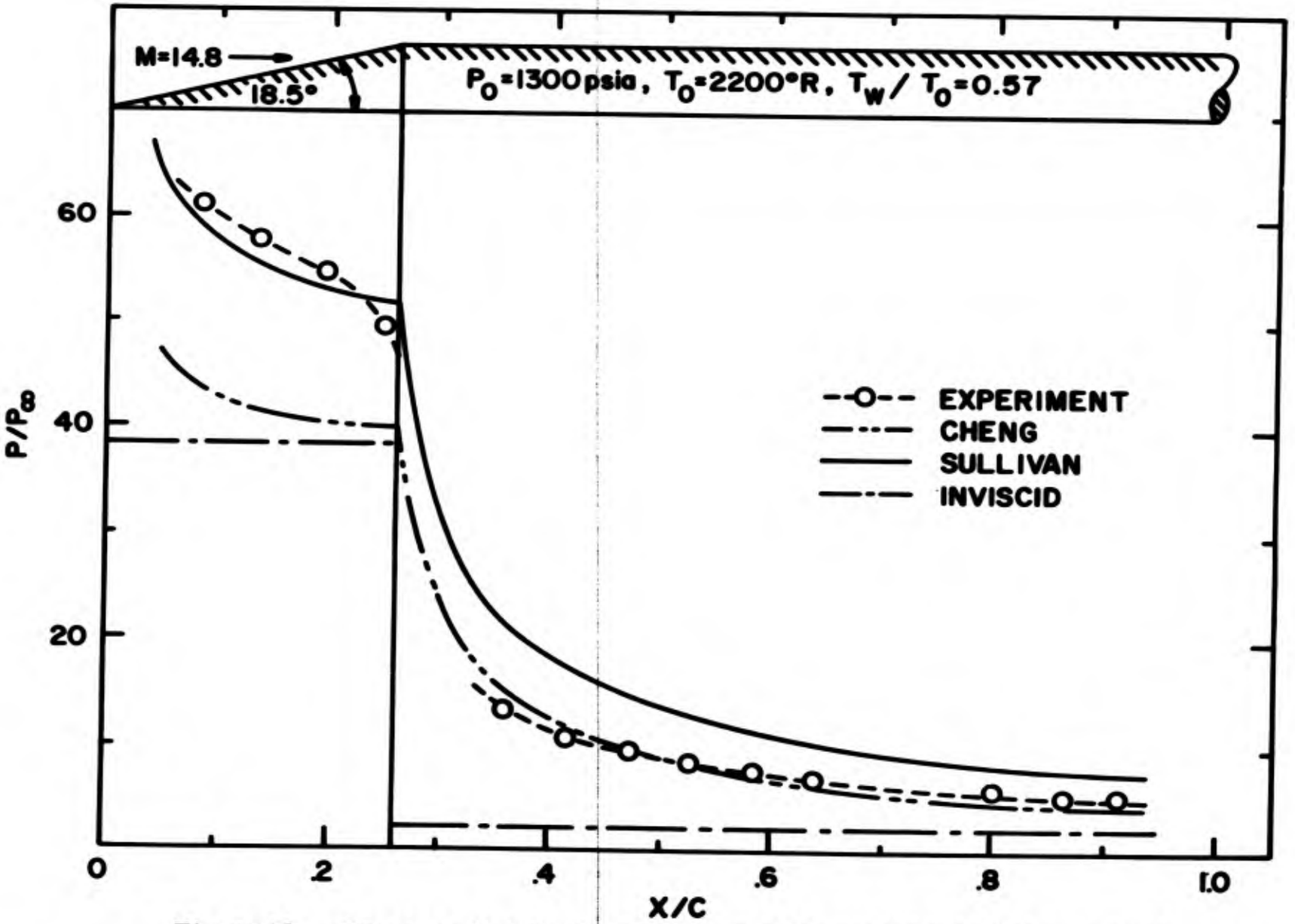

Figure 12 Pressure distribution on the expansion corner model at zero incidence: a comparison between theory and experiment (Experimental data from Ref 11).

UNCLASSIFIED

Security Classification

DOCUMENT CONTROL DATA - R & D

(Security classification of title, body of abstract and indexing annotation must be entered when the overall report is classified)

1 ORIGINATING ACTIVITY (Corporate author) Ohio State University Columbus, Ohio	2a. REPORT SECURITY CLASSIFICATION Unclassified 2b GROUP

3 REPORT TITLE

Hypersonic Viscous Interaction on Curved Surfaces

4 DESCRIPTIVE NOTES (Type of report and inclusive dates)

Scientific. Interim.

5 AUTHOR(S) (First name, middle initial, last name)

John L. Stollery

6 REPORT DATE July 1970	7a. TOTAL NO. OF PAGES 38	7b. NO. OF REFS 11
8a CONTRACT OR GRANT NO F33615-67-C-1758 b PROJECT NO 7064-00-06 c DoD Element 61102F d DoD Subelement 681307	9a. ORIGINATOR'S REPORT NUMBER(S) 9b. OTHER REPORT NO(S) (Any other numbers that may be assigned this report) ARL 70-0126	

10 DISTRIBUTION STATEMENT

1. This document has been approved for public release and sale; its distribution is unlimited.

11 SUPPLEMENTARY NOTES TECH OTHER	12 SPONSORING MILITARY ACTIVITY Aerospace Research Laboratories (ARR) Wright-Patterson AFB Ohio 45433

13 ABSTRACT

Cheng's analysis of strong viscous interaction between a laminar boundary layer growing over a flat plate and the external hypersonic flow field is extended to cover curved surfaces. It is demonstrated that the solutions for concave surfaces are oscillatory and physically unrealistic. The reason for this behavior is that the Busemann term in the Newton-Busemann pressure law used in Cheng's analysis over-corrects for centrifugal effects. The removal of the Busemann term or the substitution of the tangent-wedge pressure law results in a more realistic analysis which can cover both strong and weak viscous interaction over a variety of two-dimensional shapes. A number of examples are included together with comparative experimental data.

DD FORM 1 NOV 68 1473

UNCLASSIFIED

Security Classification

14. KEY WORDS	LINK A		LINK B		LINK C	
	ROLE	WT	ROLE	WT	ROLE	WT
Fluid mechanics						
Hypersonic flow						
Viscous interaction						